



Considering Impact and Corrosion Resistance in the Performance of Heavy Wear Resistant Coatings

CHRISTIANE SCHULZ ^{1,4} THOMAS SCHLÄFER,² JACOB PLOWMAN,^{1,3} and COLIN HALL¹

1.—University of South Australia, Adelaide, Australia. 2.—LaserBond Ltd, Sydney, Australia. 3.—University of Bath, Bath, UK. 4.—e-mail: christiane.schulz@unisa.edu.au

Laser clad coatings consisting of a Ni-based matrix and tungsten carbide (WC) hard phases are used for heavy wear protection of components in many industries. Matrix composition and WC type can be chosen to give these composites resistance to erosive/abrasive wear, as well as to the impacts of particles and corrosion. Maintaining ductility in the matrix is important, so that it can absorb impact energy and minimize cracking, thus avoiding penetration of corrosive media through cracks and subsequent corrosion in the substrate-cladding interface. Claddings were tested for their impact resistance by means of a single impact with a hard, spherical indenter. The depth of impact craters was measured, and the cracking behavior was analyzed. Corrosion resistance of Ni/WC composites, a HVOF WC/CoCr coating and a hard chrome reference coating were tested by electrochemical corrosion in a 3.5 wt.% NaCl solution and by exposure for up to 1000 h in a salt spray test.

INTRODUCTION

Parts in high-wearing applications such as pumps, pipes, and transport rolls for transporting slurry in mining and marine applications, and chisels, ploughs, and cutting blades in agriculture, require claddings to withstand impact loads and corrosion as well as typical abrasive or erosive wear.^{1–3} Currently, claddings are selected based on their performance in erosion, abrasion, and corrosion wear tests which are thought to be indicative of in-service performance. In these applications, however, claddings could be randomly impacted by rocks or other hard objects. They should, therefore, be designed to also protect against impact induced wear. Wet soil and slurries can have ions such as Cl⁻ dissolved in them, which induces an additional corrosive effect on claddings in these applications.

Laser cladding is a build-up welding process utilizing a high-powered laser to melt a powder feedstock material directly onto a metal substrate. The laser beam is focused on the work piece where, due to absorption of the beam energy, the base

material is locally heated up to its melting temperature, creating a melt pool. The powder feedstock is injected into the melt pool to form a metallurgical bond with the substrate. Laser optics and powder nozzle are moved over the work piece to deposit a uniform coating or an additively manufactured 3D part.⁴

Claddings for high wear resistance with good corrosion resistance are often composed of a Ni-based matrix with tungsten carbides as a hard phase.⁵ Such metal matrix composites (MMCs) can be applied using gas tungsten arc welding (GTAW), plasma transferred arc welding (PTAW) and laser cladding. The quality of the weld build-up in terms of dilution with the substrate and decarburization of carbides increases from the former to the latter.⁶ Self-fluxing Ni-based alloys are typically used as matrix feedstock as they combine good wear and corrosion resistance properties.⁷ WC is commonly used as a hard phase due to its good wettability by Ni-based alloys and outstanding hardness and wear resistance.⁸ Tungsten carbides can partly dissolve in the matrix during cladding, forming brittle mixed metal carbides, either as precipitates or in the form of a corona around the carbide as a result of reactions with the matrix. This effect produces a transition zone between the carbide and matrix

which gives superior metallurgical bonding of the particles.⁹ Cooling and solidification of the melt pool forms a metallurgical bond between the substrate and cladding, providing excellent adhesion.⁴ The resulting coating contains hard WC particles, providing wear resistance, cemented in a more ductile binder, which provides toughness and corrosion resistance.

By altering the composition of the pure matrices, the matrix can be designed with hardness values roughly in the range of 35–60 HRC (340–740 HV); these also show different levels of ductility. Precipitated carbides harden and embrittle the matrix.^{10,11} However, this increases the likelihood of cracking, either during the cladding process (clad cracking), or from impact suffered during service. It has been shown,^{12,13} that clad cracks initiate from residual tensile stresses and that at the cladding-substrate interface they travel preferentially through brittle phases around carbides formed from decarburization of the carbide. These carbides are referred to as η -carbides and are of the form M_6C .¹⁰ Clad cracks provide easy crack pathways for brittle fractures.¹⁴

Just et al.¹⁵ used a single impact hammer drop test at a 5 J load to compare impact resistance of Ni/WC coatings deposited by PTAW. They reported carbide decohesion and more ductility during impact in the coating with a thin carbide-matrix interphase (the corona), and a more brittle response with particle cracking in the coating with a thicker interphase, despite it having a lower matrix hardness. From this they concluded that carbide-matrix bonding plays a key role in mechanical properties of Ni/WC.

In¹⁶ a rotary impact tester was used that repeatedly impacted Ni/WC coatings, deposited by PTAW, with an 8 J load to compare impact resistance. Their report mostly showed only plastic deformation and minimal mass loss, while a few results showed chipping. They attributed good impact properties to good carbide/matrix bonding from moderate carbide dissolution, and soft matrices. To understand the deformation mechanisms involved it is worthwhile reviewing the mechanism of cracking as applied to these claddings.

When coatings are impacted by a rigid counterbody, there is localized elastic deformation around the contact area, inducing tensile stresses concentrated on the edge of the contact. On further loading a plastically deformed zone is created under the indenter. If a critical load is reached, a crack initiates at a surface defect and forms a so-called ring crack. It propagates outwards and downwards, forming a so-called cone crack. Radial cracks propagate perpendicular to the surface, driven by tensile stresses caused by subsurface deformation in the coating and substrate. Their traces can be seen on the surface, emanating radially outwards from the edges of the impact craters. Lateral cracks can be observed in cross sections, propagating parallel to

the surface under the contact area. They initiate at the deformation zone boundary, driven by residual stresses between the deformed zone and surrounding elastic zone trying to recover.¹⁷ Lawn¹⁸ explains how, with a brittle coating on a ductile substrate model, cone cracks dominate at large thickness/impact radius (d/a) values, as there is little deformation in the substrate. At d/a values of one, radial cracks dominate, initiating from the coating substrate interphase in conjunction with surface ring cracks. As d/a tends to zero, there is more effect from substrate deformation and concentric through-thickness, or 'bend induced' cracks are produced. It can be said that substrate deformation effects cause cracking at lower loads for thinner coatings with larger Young's modulus.

When the Ni/WC laser clad coatings experience an impact load, the matrix deforms by macroscopic flow, absorbing energy from the impact which can prevent cracks from forming. During this deformation, the embedded WC experience compression, which can cause their fracture before cracks appear through the matrix. If the matrix is unable to absorb sufficient impact energy, cracks initiate from stress build-up at defects or around carbides, and propagate through the coating.¹⁹

Ni/WC composites have good corrosion resistance in chloride containing solutions. However, they can only serve as a protective coating against corrosion of the substrate if they provide a dense barrier between the substrate and environment. Cracks provide a pathway for the electrolyte to penetrate to the substrate-cladding interface, where a galvanic element is formed. If the substrate material has a lower corrosion potential, E_{corr} , than the cladding material, undercorrosion occurs which can lead to catastrophic cladding failure due to delamination.

In this study several laser clad Ni/WC coatings, a WCCoCr coating produced by high velocity oxy fuel (HVOF) spraying, and a hard chrome coating were tested for their impact and corrosion resistance. Damage after a single impact from a spherical indenter was studied. Deformation and cracking behavior of Ni/WC laser clad coating with different matrix alloys and carbide types was studied for the first time. The microstructure under the impact revealed cracking for some claddings, which can have a significant influence on the corrosion resistance of the coating.

MATERIALS AND METHODS

The laser clad Ni/WC coatings were produced with two different matrix feedstock powders, denoted as Ni40 and Ni60, where 40 and 60 give the nominal hardnesses of the pure matrix material in HRC. Two types of tungsten carbides as hard phases were used; fused tungsten carbides (FTCs), or monocrystalline tungsten carbides (MTCs), the main difference between the two being phase composition. MTC consists solely of molecule WC,

whereas FTC consists of the eutectic phase of WC and W_2C . MTCs are characterized by a lower hardness and fracture toughness K_{1C} .²⁰ MTCs have a higher thermal stability, so undergo less dissolution during cladding. FTC feedstock powder can be prepared in such a way that it is spherical: sFTC denotes these types. Optical images of the laser clad cross sections were analyzed to determine volume percent of carbide and porosity. Every cladding had a carbide volume percent between 44% and 48% and porosity less than 1 vol.%. Further information on these MMCs and their erosion resistance can be found in.²¹

As references, two coatings were selected which are often used for their high wear resistance and good corrosion resistance: a HVOF sprayed WCCoCr and a hard chrome coating. HVOF is a thermal spray process in which melted and semi-melted powder particles are accelerated toward a pre-treated surface. The coating bonding mechanism is mechanical interlocking. WCCoCr is probably the most utilized wear resistant material applied with this process; the material consists of 86 wt.% WC (MTC), 10 wt.% Co, and 4 wt.% Cr. A typical coating is 100–500 μm thick and exhibits compressive stresses.²² Hard chrome is an electrodeposited layer of chrome. It is widely used in applications that involve wear and corrosion. Typical coating thickness ranges from 10 μm to 500 μm , and the residual stress regime is tensile.²²

Hardness of the matrix was measured with a micromechanical tester, Nanovea CB500, CA, USA, using a Vickers type indenter. The laser clad Ni/WC hardness values are for the matrix after cladding, given in HV0.1. A low load was used due to the limited space between carbides in the matrix. This ensured hardness was not influenced by the surrounding area. The hardness of the two reference coatings, HVOF WCCoCr and hard chrome, are given in HV0.3. For good comparability of results, the laser claddings were ground to 940–1320 μm in thickness, and the HVOF sprayed WCCoCr and hard chrome reference coatings to 220–350 μm . G250 (AS3678) mild steel was used as the substrate for all coatings.

Table I gives coating designation, coating process, tungsten carbide type and matrix/coating hardness for all investigated coatings. Matrix hardness

ranges for claddings with Ni60 were between 750 and 860 HV0.1 (60–65 HRC) and with Ni40 they were between 470 and 480 HV0.1 (47–48 HRC). Matrix hardness is higher in a laser clad Ni/WC coating than in Ni-alloy on its own due to carbide decarburization and precipitate formation. For Ni60 it can be observed that the cladding Ni60 sFTC/MTC has the lowest matrix hardness. This could be explained by the addition of 50% MTC which does not decarburize and form hard, brittle precipitates. For the two reference coatings, the overall coating hardness is given.

All samples were finely ground before testing. Impact tests were carried out by dropping a 1.8 kg weight at heights of 140 mm and 275 mm, generating impact energies of 2.5 J and 5 J, respectively. The impacting counterbody was a spherical WC–Co ball with 12.7 mm diameter. A minimum of three repeat tests were carried out for each sample at each energy. The depth of each impact crater was measured by linear profilometry using a Bruker Dektak XT, CA, USA: two profiles were measured, perpendicular to each other. The average of these values was assigned to that crater and used to calculate the average and standard deviation. Optical images of the impacts from top view and cross section were taken to determine the deformation and cracking behavior of the coating during the impact.

Electrochemical corrosion tests were conducted using a typical three-electrode setup and a Wave-driver potentiostat (Pine Research Instrumentation, NC, USA) with a solution of 3. wt.% NaCl at pH 6.8. The specimen acted as the working electrode, a saturated Ag/AgCl electrode (with a shift of +199 mV to standard hydrogen electrode) was used as a reference electrode, and a platinum wire acted as the counter electrode. Coatings were polished to mirror finish prior to testing. Open circuit potential (OCP) was measured for 45 min to allow stabilization of the system. Measurements were carried out in a naturally aerated, unstirred solution at room temperature with a mid-range scan rate of 0.25 mV/s. This scan rate allows for efficient electrochemical testing while passivation effects are still identifiable. Per sample at least 2 tests were carried out; if they were not in good agreement the test was repeated. Selected coatings had their corrosion

Table I. Coating processes and properties

Coating	Coating process	WC type	Matrix/coating hardness
Ni60 FTC	Laser cladding	FTC	810 HV0.1
Ni60 sFTC	Laser cladding	sFTC	860 HV0.1
Ni60 sFTC/MTC	Laser cladding	0.5sFTC + 0.5MTC	750 HV0.1
Ni40 sFTC/MTC	Laser cladding	0.5sFTC + 0.5MTC	480 HV0.1
Ni40 sFTC	Laser cladding	sFTC	470 HV0.1
WCCoCr	HVOF	MTC	1220 HV0.3
Hard chrome	Electrolytic	n/a	998 HV0.3

resistance assessed in a neutral salt spray test according to ISO 9227 for up to 1000 h. Samples were assessed for red rust appearance which indicated corrosion of the mild steel substrate and therefore failure of the barrier effect provided by the coating.

RESULTS AND DISCUSSION

Impact Test

Figure 1 shows the impact crater depths after 2.5 J and 5 J impacts. All samples displayed shallower craters at 2.5 J compared with 5 J. The reference coatings WCCoCr and hard chrome showed the deepest impact craters. This is mainly a result of their lower thicknesses, causing the impact to induce greater stresses and deformation in the substrate. All claddings with the harder Ni60 matrix showed shallower craters than those with the softer Ni40 matrix at both energies. This is because of the greater ductility and lower hardness of the Ni40 matrix, allowing more elastic and plastic deformation and less cracking. Impact energy is consumed when cracks form and new surfaces are created, reducing the amount of deformation of the coating-substrate system, hence lowering impact depth.

In Fig. 2 the top view and cross section micrographs after impact are displayed. The claddings containing the softer Ni40 matrix both showed only 'sink-in' damage, caused by plastic deformation of the matrix and substrate, with no cracks in their cross sections. A single crack can be seen on the surface of Ni40 sFTC; however, this is thought to

initiate from a pre-existing clad crack. In addition to sink-in damage, cross sections of claddings containing the harder Ni60 matrix also showed cone, radial, and bend induced cracks. Some traverse the thickness of the coating and were only arrested by the substrate. Lateral cracks were observed intersecting radial ones just below the plastic deformation zone in the coating. As mentioned previously, the difference in behavior is a result of the ability of the Ni40 matrix to absorb greater amounts of energy from the impact, by macroscopic flow, resulting in lower stress accumulation at weak points, preventing cracks from initiating. Both reference coatings exhibited greater damage than the laser clad coatings. Their lower thicknesses created larger impact depths which induced larger bending stresses on the surfaces of these coatings. They also have larger Young's moduli than that of the Ni/WC composites, resulting in through-thickness radial, bend, and cone cracks at lower stresses. Because hard chrome is 100 μm thinner than WCCoCr, it displayed different damage, showing a large number of through-thickness radial cracks. One reason for the different cracking behavior could be because the HVOF process induces residual compressive stresses in the coating and substrate, which serve to inhibit crack initiation. In hard chrome, however, the residual stresses are tensile, which cause tensile driven cracks to initiate and grow more easily.²²

Figure 3 shows cross sections of Ni40 sFTC/MTC and Ni60 sFTC/MTC after 5 J impact. In both claddings, MTCs have fractured from the compression of the surrounding matrix. sFTCs remain intact if they are not fractured by a crack traveling

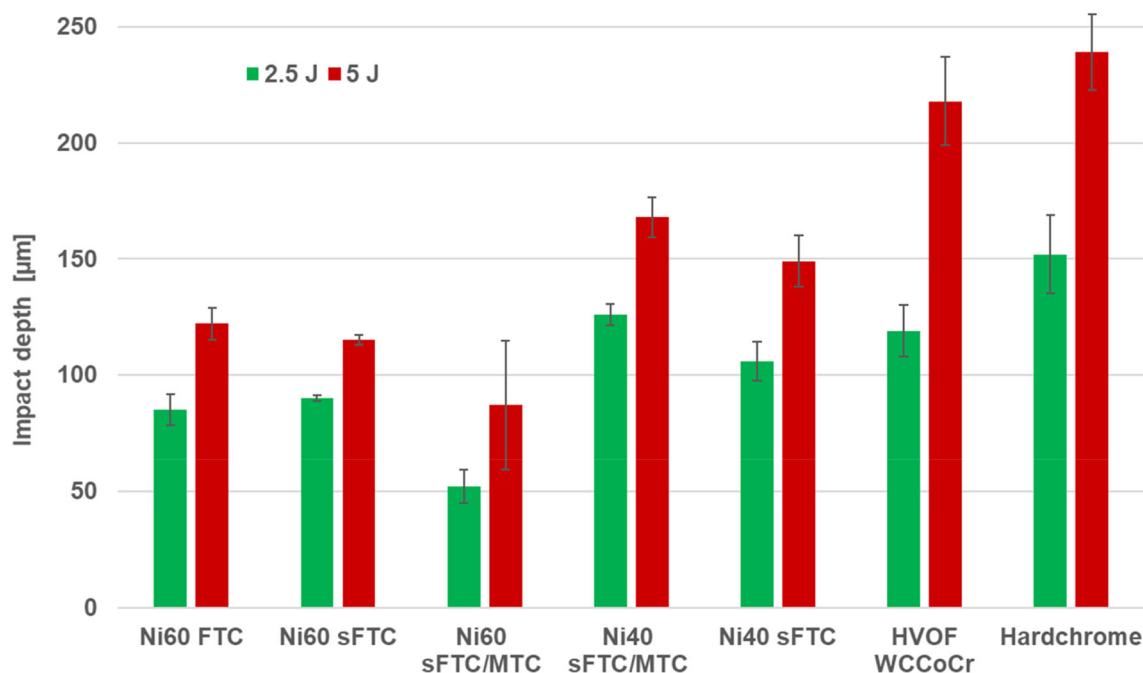


Fig. 1. Impact depth after 2.5 J and 5 J impacts.

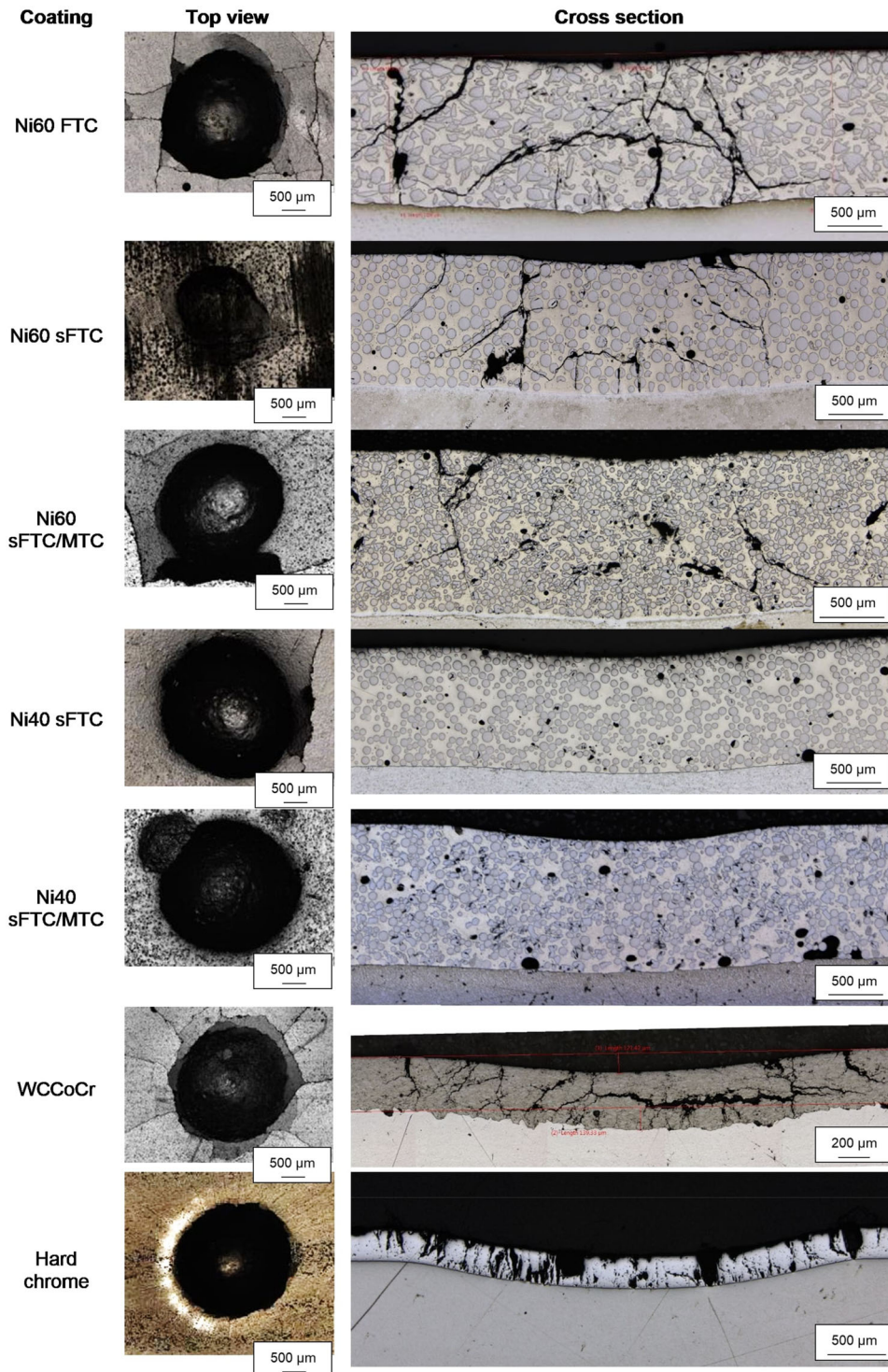


Fig. 2. Top view and cross section of coatings after impact with 5 J.

through the entire cladding. In the Ni60 clads, substituting FTC for MTC causes a reduction in impact depths at both impact energies. This effect could be explained by the MTCs absorbing some impact energy when they fracture, reducing deformation in the matrix and substrate. In the Ni40

clads, substituting FTCs for MTCs does not show a significant difference in impact depths at 5 J.

The preferential cracking of MTCs over sFTCs can be attributed to their lower fracture toughness, angular shape, and absence of a precipitated carbide phase surrounding them. Stresses become concentrated on sharp edges of the angular MTC.²³ The

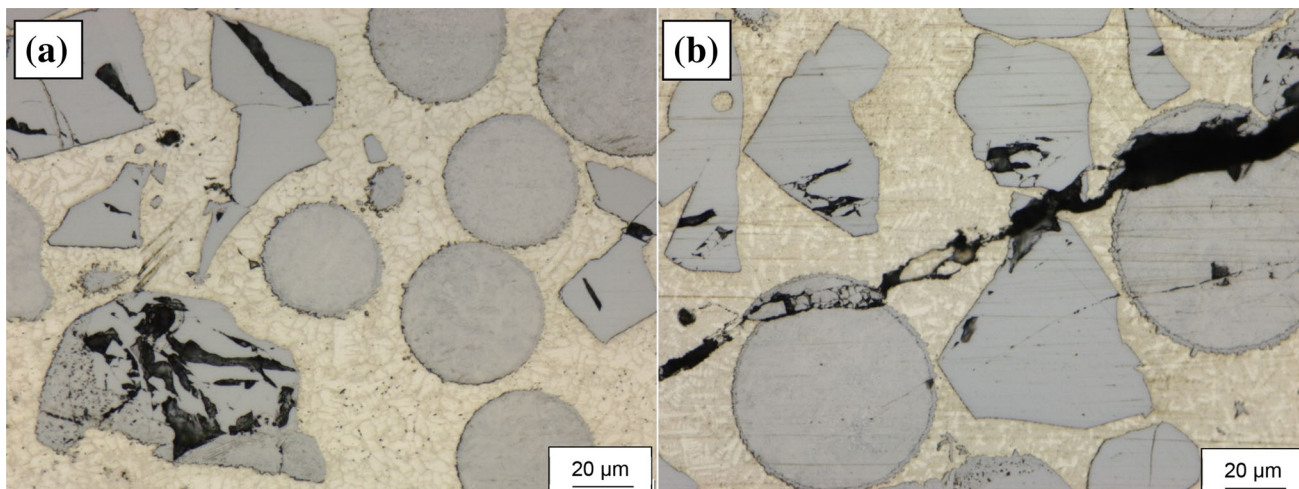


Fig. 3. Detail of (a) Ni40 sFTC/MTC after 5 J impact, and (b) Ni60 sFTC/MTC after 5 J impact.

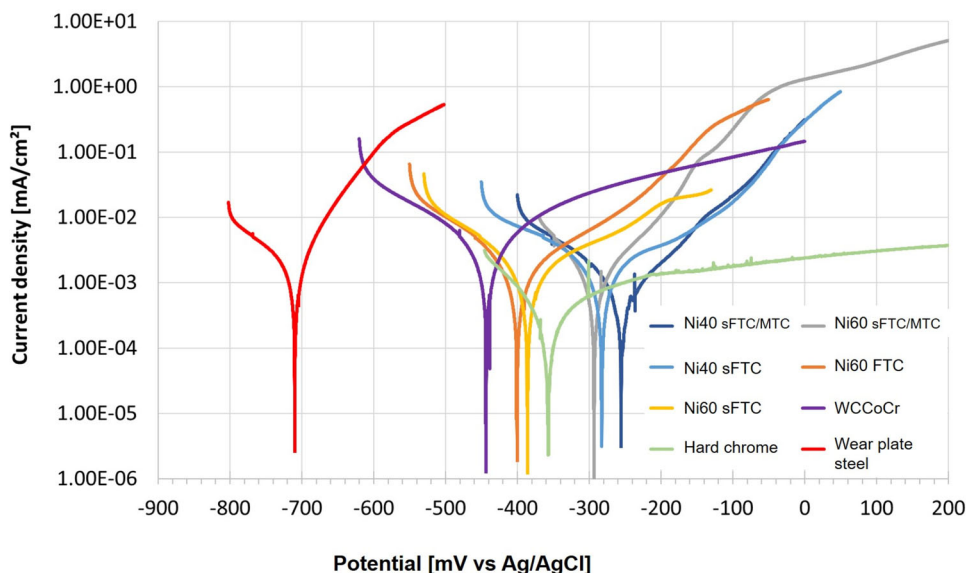


Fig. 4. Potentiodynamic corrosion in 3.5 wt.% NaCl solution.

dissolving of the carbide in the melt pool and subsequent precipitation causes a gradient to form between the carbide and matrix. This acts as a buffer by reducing the sharp change in toughness. Therefore, as the (s)FTCs have better metallurgical embedding, they show superior fracture toughness over MTCs. Complementary observations were reported by Katsich and Badisch, who concluded that a smooth carbide/matrix transition zone improves the wear behavior against volume loss due to fracture.¹¹

Corrosion Resistance

Figure 4 shows the potentiodynamic polarization curves of the investigated claddings, HVOF WCCoCr, and hard chrome references, and a wear

plate steel, Bisalloy® Wear 500. All coatings have a more noble corrosion potential E_{corr} than the wear plate steel. Corrosion current density i_{corr} , is in the same range for all materials besides hard chrome. The HVOF WCCoCr coating is the least corrosion resistant cladding of the investigated materials. It has the lowest corrosion potential E_{corr} and one of the highest corrosion current densities i_{corr} . The claddings with a Ni40 matrix seem to be more resistant in the 3.5 wt.% NaCl electrolyte than the claddings with the Ni60 matrix. This is evident from the higher corrosion potentials, E_{corr} . Corrosion resistance of the hard chrome coating was found to be superior in this experiment, showing the lowest corrosion current density i_{corr} , roughly one order of magnitude lower than that for the other coating materials. Moreover, the hard chrome coating

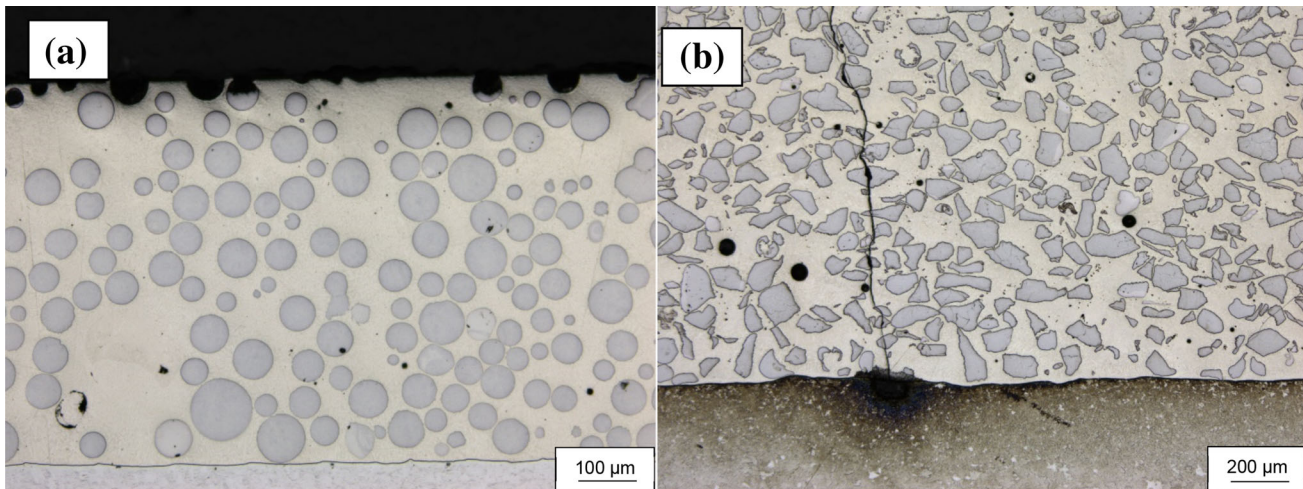


Fig. 5. (a) Ni40 sFTC after 1000 h; (b) Ni60FTC after 156 h salt spray test.

builds a stable passivation layer, so that the current increases only slightly in the anodic part of the curve. Potential was not increased to pitting potential.

Two coatings, Ni40 sFTC and Ni60 FTC, were tested for up to 1000 h in the neutral salt spray test, following ISO 9227. In this test, samples were exposed to a 5 wt.% NaCl fog at 100% humidity and 35°C. Samples were removed from the salt spray when excessive red rust formation was observed. Ni40 sFTC lasted the full 1000 h without red rust formation. Ni60 FTC, on the other hand, was removed after 156 h as heavy red rust was observed. Figure 5 shows the cross sections of Ni40 sFTC and Ni60 FTC after removal from the test after 1000 h and 156 h, respectively. The difference was attributed to the presence of through-coating clad cracks in Ni60 FTC. The electrolyte penetrated through the cracks and reached the mild steel substrate. The iron oxides formed were transported to the surface and red rust was observed on top of the coating. At the cladding-substrate interface a galvanic element formed, accelerating the degradation of the steel, ultimately leading to catastrophic coating delamination.

Therefore, cracks must be avoided to guarantee a dense barrier between coating and substrate. This includes cracks caused by impact. In applications where the surfaces can be randomly impacted by large solid objects, such as slurry pumps in mining, the cladding can crack due to these impacts (compare Fig. 2). Consequently, the barrier effect of the cladding is breached, and corrosive media can then penetrate to the substrate material and cause undercorrosion there, as in Fig. 5b, which can lead to catastrophic failure of the coating, and ultimately the entire component. The cladding material itself is fairly corrosion resistant as is evident from the potentiodynamic polarization test and no observable degradation of the cladding during the salt spray test. If cracks are avoided,

good in-service impact/corrosion resistance can be expected.

CONCLUSION

Impact resistance, in terms of cracking for laser clad Ni/WC coatings, depends greatly on hardness of the matrix material. The harder the matrix is after application of the coating, the more likely the claddings are to crack. Claddings with hard matrices always display some cracks after the cladding process due to residual stresses. Ni-based matrices are moderately corrosion resistant in 3.5 wt.% NaCl solution. However, cracks, generated during coating application or after experiencing an impact load, breach the dense barrier which would otherwise isolate the substrate from the corrosive environment. The reference coatings, hard chrome and HVOF WCCoCr, are less impact resistant than laser clad Ni/WC coatings. The corrosion resistance of the HVOF coating is slightly worse than that of the investigated claddings, while hard chrome shows somewhat better corrosion resistance. If a part experiences erosion or abrasion, as well as the likelihood of impact and moderate corrosion, a Ni/WC cladding with a soft, ductile matrix is recommended.

ACKNOWLEDGEMENTS

The CRC Program (Grant No. 53996) supports industry-led collaborations between industry, researchers and the community. We acknowledge the support of Taiho Kogyo Tribology Research Foundation (TTRF) in financing this study.

CONFLICT OF INTEREST

On behalf of all authors, the corresponding author states that there is no conflict of interest.

REFERENCES

1. R.J.K. Wood, *Wear* 261, 1012 (2006).
2. C. Schulz, T. Schläfer, B. Gilois and C. Hall. *ACA Corrosion and Protection Conference*, Melbourne, Australia, 24-27 Nov 2019.
3. A.H. Jones and P. Roffey, *Wear* 267, 925 (2009).
4. S. Nowotny, L.-M. Berger, and J. Spatzier, Coatings by Laser Cladding. *Comprehensive Hard Materials*, ed. V.K. Sarin (Amsterdam: Elsevier, 2014), p. 507.
5. J. Tuominen. Engineering Coatings by Laser Cladding—The Study of Wear and Corrosion properties. Doctoral thesis, 2009.
6. P.F. Mendez, N. Barnes, K. Bell, S.D. Borle, S.S. Gajapathi, S.D. Guest, H. Izadi, A.K. Gol, and G. Wood, *J Manuf Process* 16, 4 (2014).
7. S.F. Moustafa, Z. Abdel-Hamid, O.G. Baheig, and A. Husien, *Adv. Powder Technol.* 22, 596 (2011).
8. F. Parisa and K. Radovan, *Surf. Coat. Technol.* 276, 121 (2015).
9. P. Zhang, Y. Pang, and M. Yu, *Metals* 9, 1 (2019).
10. A. Roettger, J. Kuepferle, S. Brust, A. Mohr and W. Theisen. in *3rd International Conference on Stone and Concrete Machining*, Bochum, Germany, 2-3 November 2015.
11. C. Katsich and E. Badisch, *Surf. Coat. Technol.* 206, 1062 (2011).
12. S.W. Huang, M. Samandi, and M. Brandt, *Wear* 256, 1095 (2004).
13. S. Zhou, X. Zeng, Q. Hu, and Y. Huang, *Appl. Surf. Sci.* 255, 1646 (2008).
14. C. Lee, H. Park, J. Yoo, C. Lee, W. Woo, and S. Park, *Appl. Surf. Sci.* 345, 286 (2015).
15. C. Just, E. Badisch, and J. Wosik, *J. Mater. Process. Technol.* 210, 408 (2010).
16. R. Sundaramoorthy, S.X. Tong, D. Parekh, and C. Subramanian, *Wear* 376–377, 1720 (2017).
17. R.F. Cook and G.M. Pharr, *J. Am. Ceram. Soc.* 73, 787 (1990).
18. B.R. Lawn, *J. Mater. Res.* 19, 22 (2004).
19. J.-S. Xu, X.-C. Zhang, F.-Z. Xuan, F.-Q. Tian, Z.-D. Wang, and S.-T. Tu, *Mat. Sci. Eng. A* 560, 744 (2013).
20. O. Lanz and A. Scrivani. in *International Thermal Spray Conference & Exposition*, Orlando, FL, USA, 7-10 May 2018.
21. C. Schulz, T. Schläfer, E. Charrault, and C. Hall, *J Therm Spray Tech* 29, 520 (2020).
22. A. Ibrahim and C. Berndt. *Mater. Sci. Eng., A*, 456 (1), 114 (2007).
23. K. Van Acker, D. Vanhoyweghen, R. Persoons, and J. Vangrunderbeek, *Wear* 258, 194 (2005).

Publisher's Note Springer Nature remains neutral with regard to jurisdictional claims in published maps and institutional affiliations.